Sensing behavior of ferromagnetic shape memory Ni-Mn-Ga

Neelesh N. Sarawate[a] and Marcelo J. Dapino[a]

[a]Mechanical Engineering Department, The Ohio State University, 650 Ackerman Road, Columbus OH 43202, USA;

ABSTRACT

Due to their large magnetic field induced strains and fast response potential, ferromagnetic shape memory alloys have mainly been studied from the perspective of actuator applications. This paper presents characterization measurements on a commercial Ni-Mn-Ga alloy with a goal to investigate its feasibility as a deformation sensor. Experimental determination of flux density as a function of quasistatic strain loading and unloading at various fixed magnetic fields gives the bias field needed for maximum recoverable flux density change. This bias field is shown to mark the transition from irreversible (quasiplastic) to reversible (pseudoelastic) stress–strain behavior. A reversible flux density change of 145 mT is observed over a range of 5.8 % strain and 4.4 MPa stress at a bias field of 368 kA/m. The alloy investigated therefore shows potential as a high-compliance, high-displacement deformation sensor.

Keywords: Ferromagnetic shape memory alloy, Ni-Mn-Ga, magnetomechanical sensor

1. INTRODUCTION AND BACKGROUND

Ferromagnetic shape memory alloys in the Ni-Mn-Ga system exhibit strains of up to 10 % when exposed to magnetic fields.[1] The strain in these alloys result from the rotation of martensite twin variants in response to external magnetic fields or external stresses. Due to the magnetic field activation, Ni-Mn-Ga exhibits higher frequency response than conventional shape memory alloys.[2] The large strain and extended frequency bandwidth make these materials useful for actuator applications.[3] Consequently, the existing literature on Ni-Mn-Ga is largely focused on the effect of magnetic field on strain.[4–8] Several models have been developed which quantify the reversible and irreversible strains observed for drive configurations with uniaxial stress and field applied parallel as well as perpendicular to each other.[9–11]

The effect of external mechanical input on the magnetic behavior of Ni-Mn-Ga, or sensor effect, has received only limited attention in the literature. Mullner et al.[12] experimentally studied strain-induced changes in the flux density of a single crystal with composition $Ni_{51}Mn_{28}Ga_{21}$ under external quasistatic loading at a constant field of 0.7 T (558 kA/m). Suorsa et al.[13] reported magnetization measurements conducted on stoichiometric Ni_2MnGa material for various discrete strain and field intensities respectively ranging between 0–6 % and 5–120 kA/m. Straka and Heczko[14,15] reported superelastic response of a $Ni_{49.7}Mn_{29.1}Ga_{21.2}$ single crystal with 5M martensitic structure for fields higher than 239 kA/m and established the interconnection between magnetization and strain. Heczko[16] further investigated this interconnection and proposed a simple energy model.

The paper presents experimental measurements on the dependence of flux density with deformation, stress and magnetic field in a commercially-available Ni-Mn-Ga alloy, with a view to determining the bias field needed for obtaining maximum reversible deformation sensing as well as the associated strain and stress ranges. A reversible flux density change of 145 mT is observed over a range of 5.8 % strain and 4.4 MPa stress at a bias field of 368 kA/m.

Further author information: (Send correspondence to M.J.D.)
N.N.S.: E-mail: sarawate.1@osu.com, Telephone: 1 614 247 7480
M.J.D.: E-mail: dapino.1@osu.edu, Telephone: 1 614 688 3689

Smart Structures and Materials 2006: Active Materials: Behavior and Mechanics, edited by William D. Armstrong,
Proc. of SPIE Vol. 6170, 61701B, (2006) · 0277-786X/06/$15 · doi: 10.1117/12.658013

Downloaded From: http://proceedings.spiedigitallibrary.org/ on 07/12/2017 Terms of Use: http://spiedigitallibrary.org/ss/termsofuse.aspx

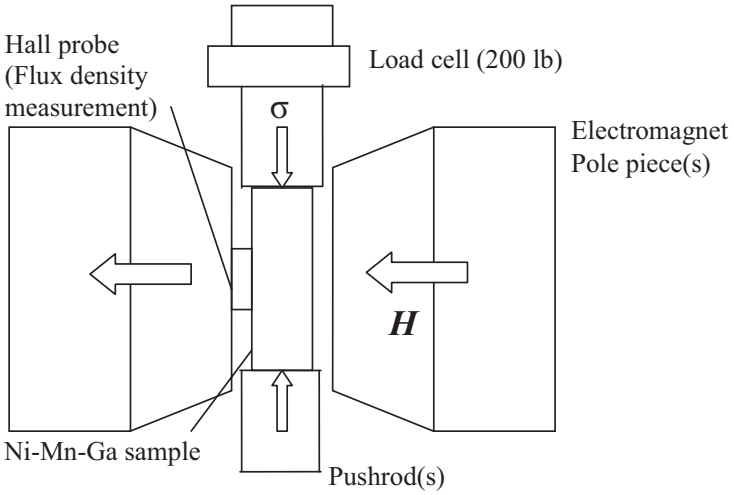

Figure 1. Experimental setup for quasistatic strain loading of Ni-Mn-Ga.

2. EXPERIMENTAL SETUP

As shown in Figure 1, the experimental setup consists of a custom built electromagnet and a loading stage. The electromagnet is made from laminated transformer steel and can produce DC and low frequency AC fields of up to 800 kA/m. It consists of two opposing E-halves which complete the magnetic flux path. Two parallel coils of about 550 turns each are mounted on the tapered center legs of opposing E-halves. The air gap of 8 mm in between the center legs is sufficient to accommodate a Ni-Mn-Ga sample and Hall probe. The variation of magnetic field in the air gap is less than 2% around the area of the pole faces. The electromagnet is powered by a 1000 VA amplifier.

A 6 x 6 x 20 mm^3 single crystal Ni-Mn-Ga sample (AdaptaMat Ltd.) is placed in the center gap of the electromagnet. The external uniaxial quasistatic strain is applied using an MTS machine with Instron controller. The sample exhibits a maximum magnetic field induced deformation of 5.8%. Initially, the sample is converted to a single field-preferred variant by applying a transverse DC field of 720 kA/m with no mechanical loading. The sample is subsequently compressed at a fixed displacement rate of 0.0254 mm/sec, and unloaded at the same rate. The flux density inside the material is measured using a Walker Scientific MG-4D Gaussmeter with a transverse Hall probe with active area 1 x 2 mm^2 placed in the gap between the magnet pole and the face of the sample. The accuracy of the method was confirmed by FEMM software. The small air gap ensures that the flux density inside the sample and that acting on the probe are equal. The compressive force is measured by a 200 lb load cell, and the displacement is measured by an LVDT. The externally applied field is obtained from the calibration curve of the electromagnet as a function of the measured current. This process is repeated under varying magnitudes of bias fields ranging from 0-479 kA/m.

3. RESULTS

3.1. Stress-Strain Behavior

Figure 2 shows stress vs. strain curves at varied bias fields, in which the expected magnetoelastic behavior of Ni-Mn-Ga is observed.[12,14] The applied transverse field results in orientation of crystals with their magnetically easy c-axis in the transverse direction, which causes the sample to elongate in the longitudinal direction. This is a consequence of growth of "field-preferred" martensite variants with the c-axis aligned with the external magnetic field. Application of compressive stresses favors the growth of "stress-preferred" twin variants with the c-axis in the longitudinal direction. Thus, in this configuration magnetic fields and stresses create competing effects.

Downloaded From: http://proceedings.spiedigitallibrary.org/ on 07/12/2017 Terms of Use: http://spiedigitallibrary.org/ss/termsofuse.aspx

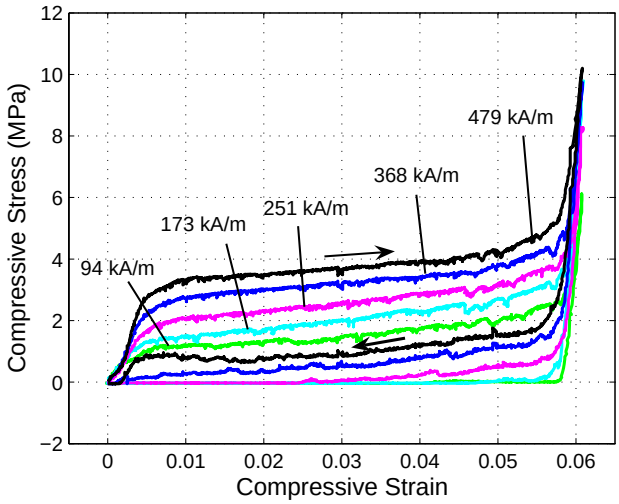

Figure 2. Stress-strain curves of Ni-Mn-Ga under different magnetic fields.

Because the twin variants are not mobile during initial compression below the detwinning stress (3 MPa in this case), the sample exhibits a relatively high stiffness in this region. With further application of stress, the rearrangement of twin variants, i.e., growth of stress-preferred variants at the expense of field preferred variants, continues resulting in a low stiffness region. This rearrangement continues until the sample is converted to one variant preferred by stress. When the sample is loaded further, it follows the steeper region indicating high stiffness after the twin rearrangement has been completed.

The stress-strain behavior varies with applied magnetic field. As the effect of stress is opposite that of the applied field, the detwinning stress increases with increasing bias fields. The external stress has to do more work at higher applied fields to initiate the rearrangement of twin variants. The detwinning stress is a characteristic of the specimen, and is an important parameter for model development.[17]

During unloading, the stress-strain curves show reversible or irreversible behavior depending on the magnitude of bias field. At low fields, the sample does not return to its original shape. The stress-induced deformation in the longitudinal direction remains almost unchanged. This is because the magnetic energy is not high enough to initiate the redistribution of twin variants. This irreversible behavior is also termed as quasiplastic behavior. This effect is analogous to the actuation effect under no or small load, when the field induced strain in the sample remains even after the field is removed. In that case, the stress is not strong enough to initiate growth of stress-preferred variants to bring the sample to its original length.

At high bias fields, the sample exhibits reversible behavior known as magnetic field induced superelasticity or pseudoelasticity. The magnetic energy is high enough to nucleate the growth of field-preferred variants when the sample is unloaded. Again, this is analogous to actuation under moderate stress when the sample returns to its original dimensions after every cycle resulting in reversible actuation. For the intermediate bias fields, the material exhibits partial recovery. The field is strong enough to initiate growth of field-preferred variants but not strong enough to achieve complete strain recovery.

3.2. Flux Density Dependence on Strain and Stress

The flux density plots shown in Figures 3–4 are of interest for sensing applications. The absolute value of flux density decreases with increasing compressive stress. As the sample is compressed from its initial field-preferred variant state, the stress-preferred variants are nucleated at the expense of field-preferred variants. Due to the high magnetocrystalline anisotropy of Ni-Mn-Ga, the nucleation and growth of stress-preferred variants occurs in concert with rotation of magnetization vectors into the longitudinal direction, which causes a reduction of the permeability and flux density in the transverse direction.

Downloaded From: http://proceedings.spiedigitallibrary.org/ on 07/12/2017 Terms of Use: http://spiedigitallibrary.org/ss/termsofuse.aspx

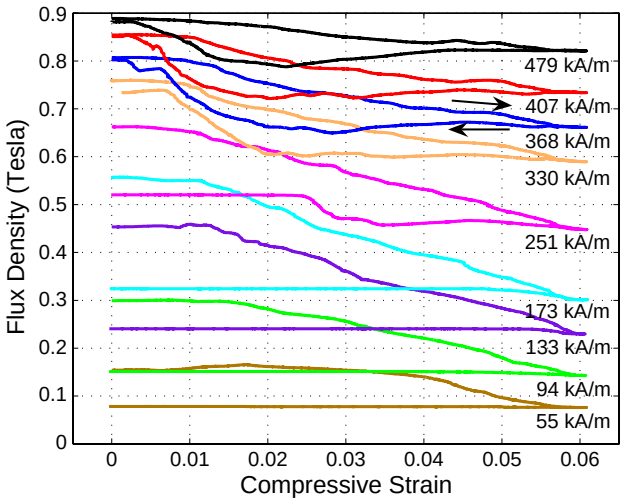

Figure 3. Flux density vs compressive strain as a function of varied bias fields.

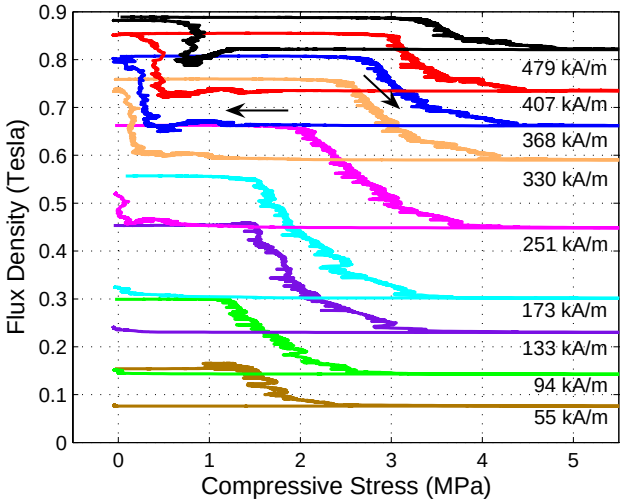

Figure 4. Flux density vs compressive stress as a function of varied bias fields.

Downloaded From: http://proceedings.spiedigitallibrary.org/ on 07/12/2017 Terms of Use: http://spiedigitallibrary.org/ss/termsofuse.aspx

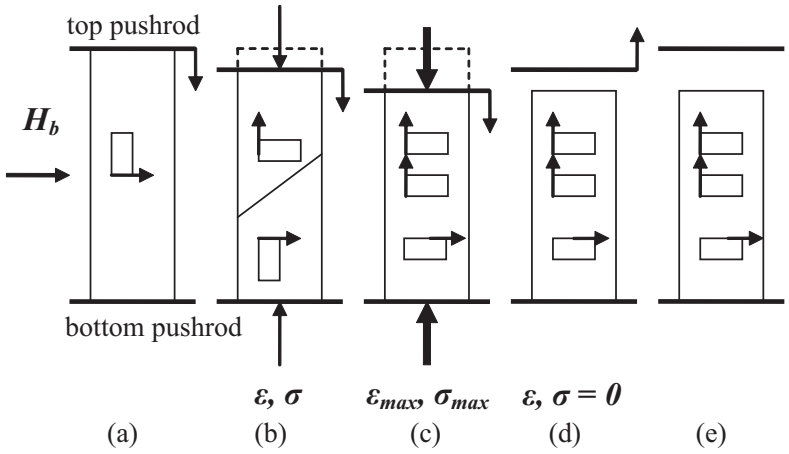

Figure 5. Schematic of loading and unloading at low magnetic fields.

4. DISCUSSION

4.1. Magnetic Field Induced Stress and Flux Density Recovery

There is a close correlation between Figure 2 and Figures 3- 4 regarding the reversibility of the magnetic and elastic behaviors. The change in flux density relative to the initial field-preferred single variant is directly associated with growth of stress-preferred variants. Thus, the flux density value returns to its initial value only if the stress vs. strain curve exhibits magnetic field induced pseudoelasticity. This occurs for this alloy at bias fields of 368 kA/m and higher. At high bias fields, the magnetic energy is high enough to initiate and complete the redistribution of variants relative to the single stress-preferred variant formed at maximum compression, during unloading. During this redistribution the magnetization vectors rotate into the transverse direction, resulting in recovery of flux density to its original value along with pseudoelastic recovery. At fields of 94 kA/m or lower, the magnetic field energy is not strong enough to initiate redistribution of variants. Hence the flux density remains unchanged while the sample is unloaded. Correspondingly the stress vs. strain curve also shows irreversible (quasiplastic) behavior.

Figures 5 and 6 illustrate this mechanism in more detail. Figure 5 illustrates the compression of a simplified, two-variant FSMA structure at low bias fields. Before the compression cycle commences, a high transverse field is applied to transform the sample to a single field-preferred variant. In this configuration, all magnetization vectors align themselves in the direction of the field. When a low bias field is applied, the magnetization vectors reorient to form 180-degree stripe magnetic domains which results in lower net flux density. The magnetization vectors remain in the transverse direction, and since no external stress is applied, the field-preferred variant configuration remains intact.

The compression starts at this maximum sample length, with comparatively low net flux density, panel (a). With increasing compression, the stress-preferred variants nucleate and grow. The variant nucleation is associated with rotation of magnetization vectors into the longitudinal direction, as they are attached to c-axis due to high magnetocrystalline anisotropy. This results in reduction in flux density in transverse direction, panel (b). The sample is entirely converted to stress-preferred state, but few magnetization vectors remain in the horizontal (hard) direction depending on the field strength, panel (c). When the sample is unloaded, the magnetic field energy is not high enough to initiate redistribution of variants into a single field-preferred variant state, panel (d). Hence, there is little or no change in the flux density value after unloading, panel (e), which corresponds with the fact that the stress-strain and flux density plots do not show any recovery for fields lower than 94 kA/m.

Downloaded From: http://proceedings.spiedigitallibrary.org/ on 07/12/2017 Terms of Use: http://spiedigitallibrary.org/ss/termsofuse.aspx

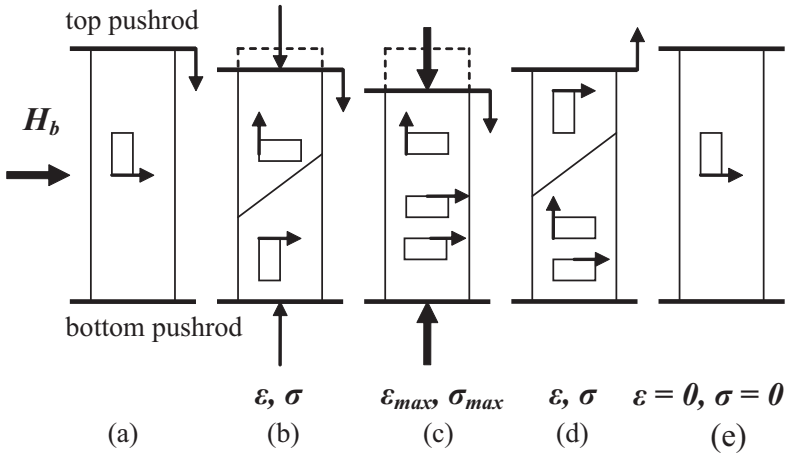

Figure 6. Schematic of loading and unloading at high magnetic fields.

Figure 6 illustrates the effect of stress loading and unloading at high bias fields. The initial net flux density is high when the sample is at its maximum length, panel (a). As in the earlier case, there is a reduction in the transverse flux density with increasing compression, panel (b). When the sample is converted to single stress-preferred variant state, some magnetization vectors remain in the transverse direction as the bias field is large enough to force magnetic moments to break away from the c-axis, panel (c). When the unloading starts, the available magnetic energy is high enough to cause nucleation and growth of field-preferred variants, while forcing the magnetization vectors to rotate into the transverse direction. Thus, the sample starts elongating again, and the expanding sample tries to force on the pushrods resulting in increasing compressive stress, panel (d). When the sample is near zero deformation, the field is high enough to induce complete variant rearrangement, the sample returns to its original structure thus exhibiting pseudoelastic behavior, and the original value of flux density is also recovered, panel (e). Thus, the magnetic field induced pseudoelasticity occurs in concert with the recovery of flux density.

This correlation can also be realized from the Figure 4, where it can be seen that the flux density-stress curves bear a resemblance to the conventional magnetic field induced strain curves.[10] Under low stresses, the strain-field plots show irreversible behavior, whereas at higher stresses the behavior is reversible. If the stress is very high (higher than the blocking force), the material shows no field induced deformation as the applied stress will be too high to allow variant rearrangement. Similarly, if the applied bias field is very high (higher than the saturation field), there will not be any change in flux density even when the sample is completely compressed. This is because the magnetic field will be too high to allow rotation of magnetization vectors in a direction perpendicular to it. An optimum compressive stress is needed to achieve maximum field induced deformation for actuation applications. Similarly, an optimum bias field is required to achieve maximum flux density change for sensing applications.

4.2. Optimum Bias Field for Sensing

The flux density starts changing when the initial detwinning stress is reached and continues to change until the final detwinning stress is reached, with all variants being transformed to one variant preferred by stress. The magnitude of total change in flux density during compression can be defined as sensitivity. The sensitivity is found to initially increase with increasing bias fields and then decrease after reaching a maximum at 173 kA/m (Figure 7). However, the reversible behavior required for sensing applications is observed at bias fields of 368 kA/m and higher. Thus, 368 kA/m can be defined as optimum field for sensing applications.

Downloaded From: http://proceedings.spiedigitallibrary.org/ on 07/12/2017 Terms of Use: http://spiedigitallibrary.org/ss/termsofuse.aspx

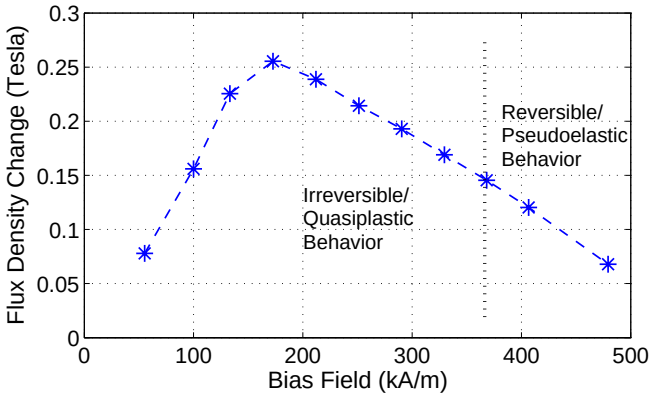

Figure 7. Flux density change as function of bias field.

This behavior can be explained from the easy-axis and hard-axis magnetization curves for this alloy shown in Figure 8. The easy-axis curve refers to magnetization of material along its easy axis (c-axis). It was obtained by first converting the sample to a single field-preferred variant and subsequently exposing it to a 0.5 Hz sinusoidal transverse field while leaving it mechanically unconstrained. The easy axis magnetization curve has a steeper slope, and it tends to saturate at low fields, about 120 kA/m in this case. The hard-axis curve refers to magnetization of material along its hard axis (other than the c-axis). To obtain the hard-axis curve, the sample was first converted to a single stress-preferred variant. Then the sample having all variants with c-axis in longitudinal direction was subsequently exposed to a 0.5 Hz sinusoidal field while being prevented from expanding. This means that the sample was magnetized along an axis other than the c-axis i.e. the hard axis. The hard axis magnetization curve has a lower slope with higher saturation field, 640 kA/m for this alloy. To magnetize the sample along hard axis, the externally applied field has to overcome the anisotropy energy to rotate the magnetization vectors away from the c-axis which is perpendicular to field. The mechanical constrains ensure that the field-preferred variants do not nucleate, thus maintaining the c-axis along longitudinal axis.

At maximum elongation for a given bias field, the flux density value is that corresponding to the easy axis value. When the sample is compressed at a constant field the induction value changes from the corresponding easy axis value to the corresponding hard axis value. Compression at constant field corresponds to a straight line starting at easy axis curve and ending at the hard axis curve. Therefore at maximum compression, with all variants being stress-preferred, the hard axis value is the lowest flux density at given bias field.

Hence, the maximum flux density change occurs when the two curves are at maximum vertical distance from each other. A large flux density change of 230 mT is observed at a bias field of 173 kA/m. However, the optimum sensing range for reversible sensing behavior occurs when the two curves are at maximum distance from each other and the sample shows pseudoelastic behavior. At a bias field of 368 kA/m, a reversible flux density change of 145 mT is obtained over a range of 5.8 % strain and 4.4 MPa stress.

5. CONCLUDING REMARKS

A reversible flux density change of 145 mT is observed over a range of 5.8 % strain and 4.4 MPa stress at a bias field of 368 kA/m. By way of comparison, Terfenol-D exhibits a higher maximum sensitivity of 0.4 T at a lower bias field of 16 kA/m and higher stress range of 20 MPa[18] However, the associated deformation is only 0.1 % due to the higher Terfenol-D stiffness. The Ni-Mn-Ga alloy investigated here therefore shows potential for high-compliance, high-displacement deformation sensors.

Downloaded From: http://proceedings.spiedigitallibrary.org/ on 07/12/2017 Terms of Use: http://spiedigitallibrary.org/ss/termsofuse.aspx

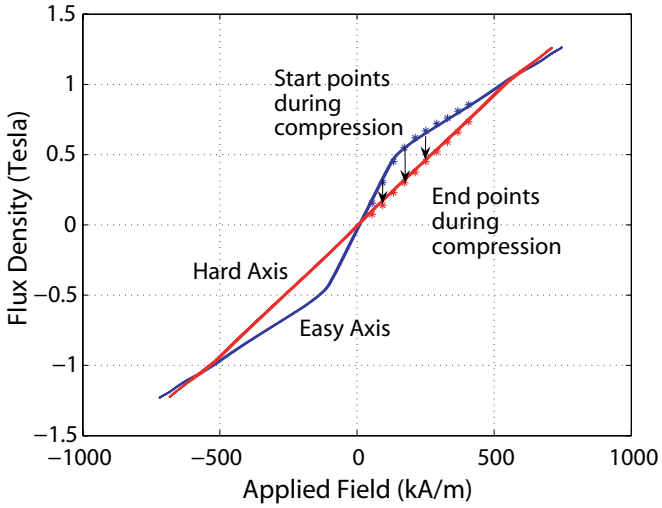

Figure 8. Easy and hard axis flux density curves of Ni-Mn-Ga.

REFERENCES

1. A. Sozinov, A. Likhachev, N. Lanska, and K. Ullakko, "Giant magnetic field induced strain in Ni-Mn-Ga seven-layered martensitic phase", *Applied Physics Letters*, **80** (10), March 2002.
2. L. Faidley, M. Dapino, G. Washington, T. Lograsso, "Dynamic response in the low-kHz range and delta-E effect in ferromagnetic shape memory Ni-Mn-Ga", *Proceedings of IMECE* (43198), 2003.
3. I. Suorsa, E. Pagounis, K. Ullakko, "Magnetic shape memory actuator performance", *Journal of Magnetism and Magnetic materials*, 272-276, pp. 2029-2030, 2004.
4. K. Ullakko, J. Huang, C. Kantner, R. O'Handley, and V. Kokorin, "Large magnetic-field-induced strains in Ni2MnGa single crystals," *Applied Physics Letters*, **69**, pp. 1966-1968, September 1996.
5. R. O'Handley, "Model for strain and magnetization in magnetic shape-memory alloys", *Journal of Applied Physics*, **83** (6), pp. 3263-3270, March 1998.
6. S. Murray, M. Marioni, S. Allen, R. O'Handley, and T. Lograsso, "6% magnetic field induced strain by twin boundary motion in ferromagnetic Ni-Mn-Ga", *Applied Physics Letters*, **77** (6), pp. 886-888, August 2000.
7. C. Henry, D. Bono, J. Feuchtwanger, S. Allen, and R. O'Handley, "AC field induced actuation of single crystal Ni-Mn-Ga", *Journal of Applied Physics*, **91** (10), pp. 7810-7811, May 2002.
8. L. Faidley, M. Dapino, G. Washington, T. Lograsso, and R. Smith, "Analytical and experimental issues in Ni-Mn-Ga transducers", *Proceedings of SPIE Smart Structures and Materials* 2001, 4327, pp. 521-532, Newport Beach, CA, 4-8 March 2001.
9. S. Murray, M. Marioni, A. Kukla, J. Robinson, R. O'Handley, and S. Allen, "Large field induced strain in single crystalline Ni-Mn-Ga ferromagnetic shape memory alloy", *Journal of Applied Physics*, **87** (9), pp. 5774-5776.
10. A. Likhachev, K. Ullakko, "Magnetic field controlled twin boundaries motion and giant magneto-mechanical effects in Ni-Mn-Ga shape memory alloy", *Applied Physics Letters*, **275**, pp. 142-151, October 2000.
11. L. Faidley, M. Dapino, G. Washington, "Strain model for Ni-Mn-Ga with collinear field and stress", *Proceedings of IMECE* 2005, Orlando, FL, November 2005.
12. P. Mullner, V. Chernenko, and G. Kostorz, "Stress-induced twin variant rearrangement resulting in a Ni-Mn-Ga ferromagnetic martensite", *Scripta Materialia*, **49**, pp. 129-133, 2003.
13. I. Suorsa, E. Pagounis, and K. Ullakko, "Magnetization dependence on strain in the Ni-Mn-Ga magnetic shape memory material", *Applied Physics Letters*, **84** (23), pp. 4658-4660, June 2004.
14. L. Straka, and O. Heczko, "Superelastic response of Ni-Mn-Ga martensite in magnetic fields and a simple model", *IEEE Transactions on Magnetics*, **39** (5), pp. 3402-3404, September 2003.

Downloaded From: http://proceedings.spiedigitallibrary.org/ on 07/12/2017 Terms of Use: http://spiedigitallibrary.org/ss/termsofuse.aspx

15. L. Straka, and O. Heczko, "Reversible 6 % strain of Ni-Mn-Ga martensite using opposing external stress in static and variable magnetic fields", *Journal of Magnetism and Magnetic Materials*, **290-291** (2), pp. 829-831, 2005.
16. O. Heczko, "Magnetic shape memory effect and magnetization reversal", *Journal of Magnetism and Magnetic Materials*, **290-291**, pp. 787-794, 2005.
17. R. Couch, I. Chopra, "A quasi-static model for Ni-Mn-Ga magnetic shape memory alloy", *Proceedings of SPIE Smart Structures and Materials* 2005.
18. R. Kellog, "The Delta-E effect in terfenol-D and its applications in a tunable mechanical resonator", M.S. Thesis, Iowa State University, Ames, 2000.

Downloaded From: http://proceedings.spiedigitallibrary.org/ on 07/12/2017 Terms of Use: http://spiedigitallibrary.org/ss/termsofuse.aspx